Chapter 4 Result and Discussions

MICROSTRUCTURAL, PHYSICAL, AND MECHANICAL BEHAVIOUR OF SINTERED ALLOY

4.1 Introduction

The present study is aimed to evaluate the impact of alloying both niobium and copper with titanium for biomedical applications, especially dental implants. It was reported earlier that titanium with 5% copper gives excellent hardness properties, antibacterial activity, lower elastic modulus, and good cytocompatibility (J. Liu et al., 2014). Thus, the Ti-5Cu-x%Nb alloy has been prepared with the addition of varying concentrations of niobium by powder metallurgy route. The XRD study of milled powder and sintered alloy, microstructural properties, elemental mapping of elements, and physical and mechanical properties is discussed in this chapter.

4.2 Phase identification and microstructure characterization

Figures 4.1 and 4.2 show the XRD pattern of the high-energy ball-milled alloy powder and sintered alloy of S1, S2, S3, and S4, respectively. The mixed ball-milled powder XRD pattern clearly shows the distinct peak of titanium (JCPDS reference no 00-044-1294), copper (01-089-2838), and niobium (00-002-1108). This shows that the alloy powder was mixed in a non-reactive manner, with no additional compound formed between the metal powders. Besides these, the XRD patterns of sintered alloys (S1-S4) show peaks of α- titanium, β-titanium, and compound of copper and titanium. With increasing niobium content, the proportion of β-phase of titanium increases, and a major peak is observed for sample S4 having (maximum percentage of Nb) as shown in Fig. 4.2 (d). The binary phase diagram of titanium-copper and titanium-niobium suggests that at 900 ºC, only solid-state fusion takes place between the powder. Titanium in both phases (α and β) can be observed in the XRD pattern of S2, S3, and S4.

In Fig. 4.2, alloy S1 has peaks of alpha Ti and Ti_2Cu intermetallic compound, whereas samples

S2, S3, and S4 have peaks for alpha Ti, Ti_2Cu, and beta Ti. In the XRD pattern of the sintered alloy at 38.5 (2θ degree), it is observed that with an increasing amount of niobium, the peak also increases gradually, and major peaks were observed for sample S4. This is because of the formation of the β- phase with increasing niobium percentage in the alloy. All the major and minor peaks of sintered alloy are analyzed by X'pert High Score Plus software and match with reference JCPDS No (00-044-1288, 00-044-1294, 01-072-0441). The average crystalline size and lattice strain were also calculated using the XRD pattern for the milled powder and sintered alloys as listed in Tables 4.1 and 4.2, respectively. The lowest value of the crystalline size of alloy S4 revealed that the sintering temperature is adequate (Ruys A, 2019). The volume fraction of the β-phases in the sintered alloys also increases from S2 to S4 and the highest 28.2 % was observed for S4, as listed in Table 4.3. This shows that the Nb stabilizes the β- phases in the alloys (Ehtemam-Haghighi et al., 2016). The major and minor peaks of titanium and compound Ti_2Cu match, and the XRD diffraction peak of titanium and niobium alloys match exactly with previous research (Han et al., 2015).

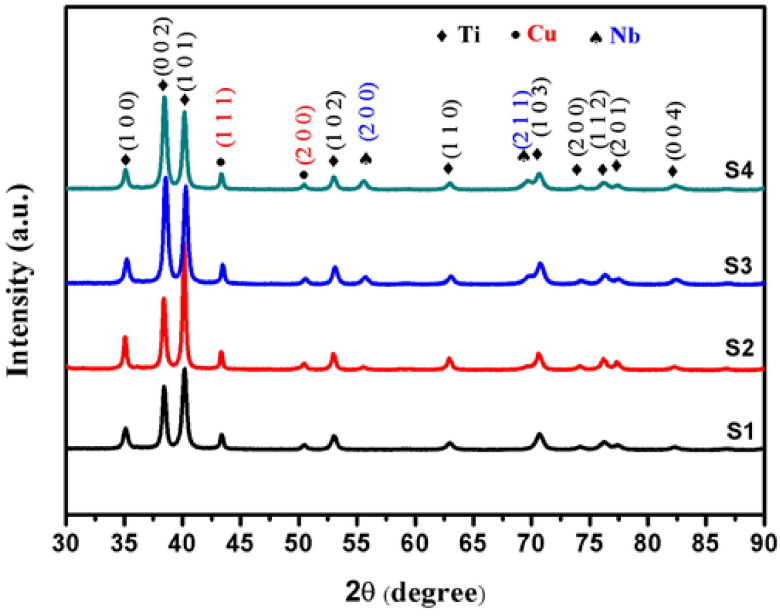

Figure 4.1- *XRD pattern of S1, S2, S3, and S4 alloy powder after ball milling.*

Table 4.1- Average crystalline size (angstrom) and average lattice strain (percentage) of ball-milled powder

Milled Powder	Ti		Cu		Nb	
	Average crystalline size (Å)	Average lattice strain (%)	Average crystalline size (Å)	Average lattice strain (%)	Average crystalline size (Å)	Average lattice strain (%)
S1	197 ± 44.3	0.41±0.07	312 ± 131.5	0.364±0.094	-	-
S2	317±102.5	0.28±0.05	433±227	0.289±0.095	166	0.503
S3	194.9±63.9	0.47±0.09	315±111.1	0.353±0.071	166	0.501
S4	217.4±78.1	0.44±0.08	322±101.8	0.345±0.056	151.50±38.89	0.50±0.05

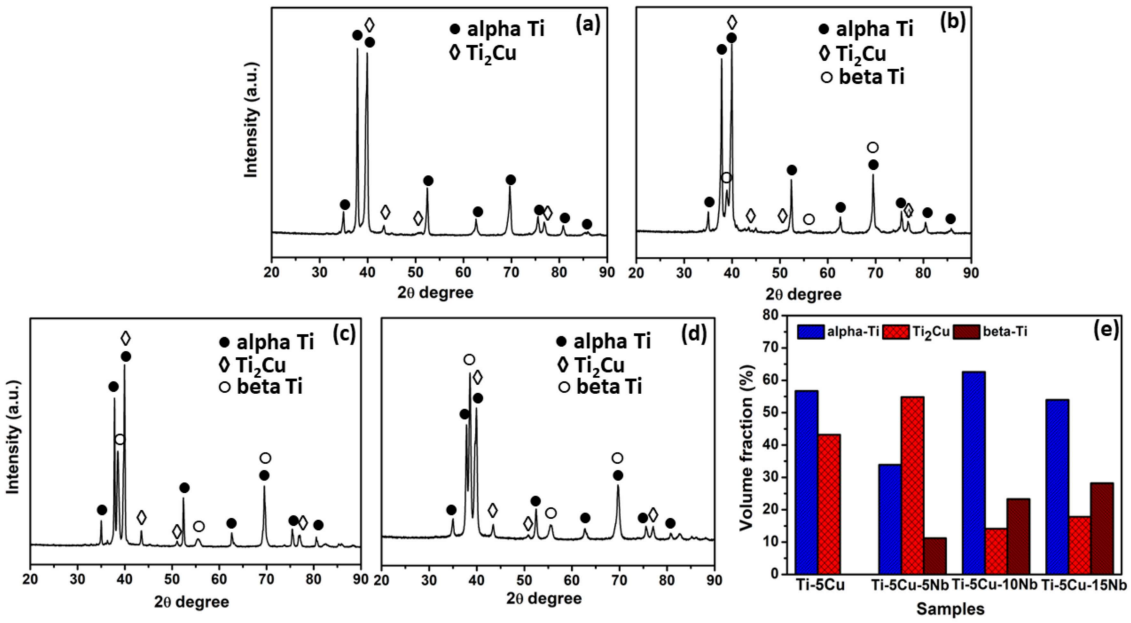

Figure 4.2- XRD pattern of (a) S1, (b) S2, (c) S3, (d) S4, and (e) volume fraction of formed phases after sintering.

Table 4.2- Average crystalline size (angstrom) and average lattice strain (percentage) of sintered alloys.

Sintered Alloys	α -Ti		Ti_2Cu		β -Ti	
	Average crystalline size (Å)	Average lattice strain (%)	Average crystalline size (Å)	Average lattice strain (%)	Average crystalline size (Å)	Average lattice strain (%)
S1	430.20±250.84	0.28±0.09	312.80±35.65	0.30±0.09	-	-
S2	446.50±96.39	0.28±0.06	374.83±36.56	0.21±0.07	300.33±269.04	0.48±0.39
S3	425.37±343.58	0.33±0.17	559.25±191.28	0.20±0.08	472.20±183.96	0.254±0.18
S4	256.85±98.32	0.41±0.15	317.5±72.65	0.34±0.14	231.66±46.92	0.39±0.12

Table 4.3- Volume fraction of phases in the sintered alloys.

Sintered Alloys	α-Ti (%)	Ti_2Cu (%)	β-Ti (%)
S1	56.70	43.21	-
S2	33.90	54.80	11.20
S3	62.58	14.13	23.28
S4	53.96	17.82	28.20

Figure 4.3 shows an optical microscopy image of the sintered alloys S1, S2, S3, and S4. The figure shows the formation of α'' phase and β- phase with increasing niobium content. Figure 4.4 is the high-resolution image of the microstructure of all sintered alloys. In Fig. 4.4 (a), the absence of the pore indicates maximum sintered density. Also, the maximum grey phase is visible, which shows the presence of α-titanium (J. Liu et al., 2014). The white phase indicates the presence of a copper-rich Ti_2Cu phase. Figures 4.4 (c) and (d) have different microstructures compared to the previous ones. The presence of niobium stabilizes the β-phase of titanium, and the dark grey phase of the hexagonal titanium and laminate structure of α''-

titanium can easily be observed. The laminate has a needle-like arrangement in Fig. 4.4 (c and d) is visible. The acicular shape or needle-like form shows the formation of the α"-phase, which is a typical phase obtained during the sintering of titanium with Nb and Sn (Ehtemam-Haghighi et al., 2016). In earlier research, the effect of niobium on the microstructure of titanium was shown to be approximately the same as in this research (Han et al., 2015). The dark grey phase and light grey phase indicate the presence of β and α phases of titanium. The laminate structure increases with an increasing percentage of niobium. In Figure 4.4 (d), the niobium is 15%, and its microstructure reveals the same. Because of the fixed amount of copper in the alloy, the quantity of the Ti_2Cu phase is almost the same in all of them.

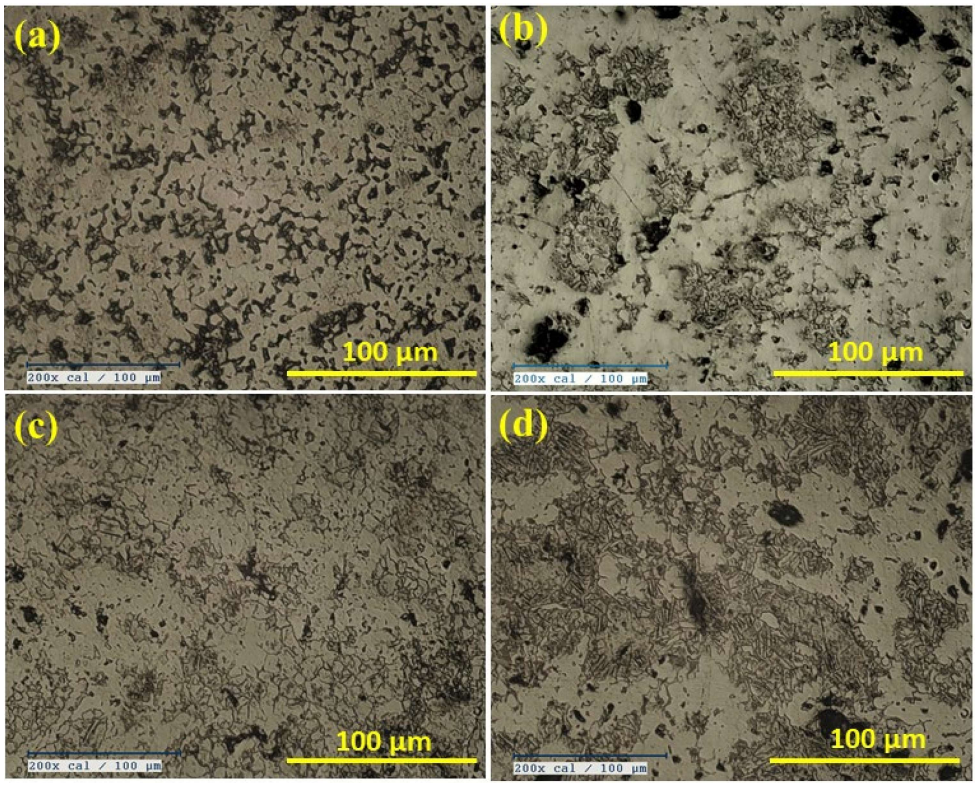

Fig. 4.3 - Optical microscopy image of sintered alloy (a) S1, (b) S2, (c) S3, (d) and S4.

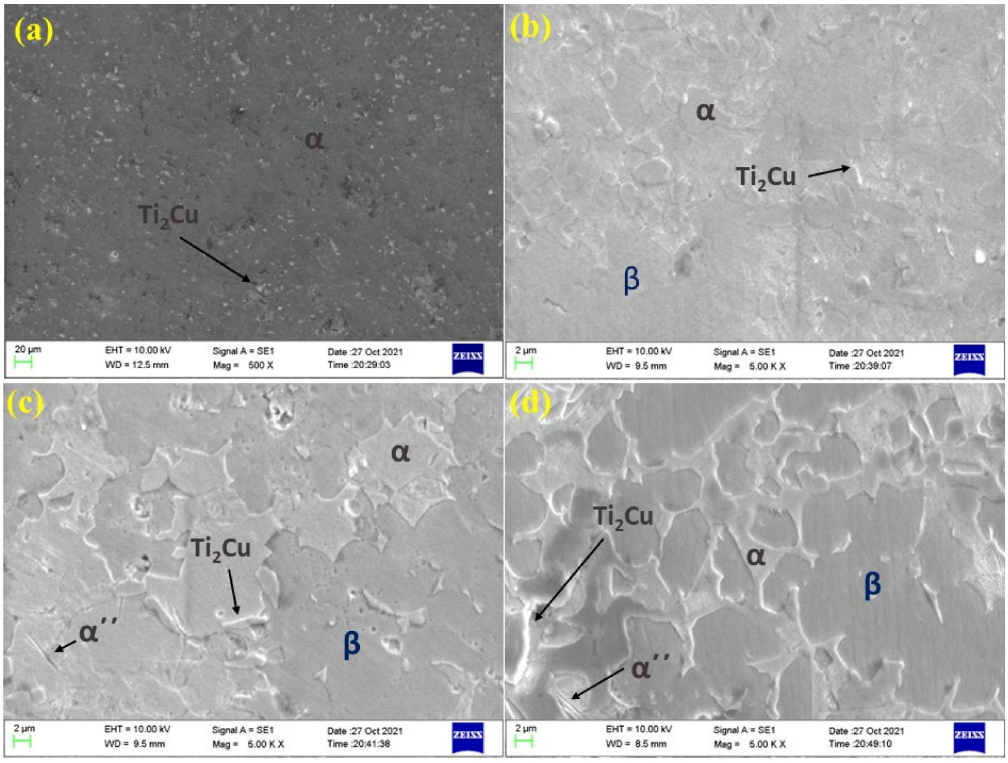

Fig. 4.4 – The scanning electron microscopy image of sintered alloy, (a) S1, (b) S2, (c) S3, and (d) S4.

Figure 4.5 shows the EDS and elemental mapping of alloy S1 at a particular surface area. In Fig. 4.5 (a), grey and the dark whitish phase can be easily observed along the grain boundary shown in the block-like structure. At this particular position, the EDS analysis confirms the presence of both titanium and copper. The distribution of titanium and copper element is observed in the mapping image, as shown in fig. 4.5 (b) and (c). The weight and atomic distribution are also shown in Fig. 4.5 (d).

The EDS analysis and elemental distribution of polished and chemically etched alloy S2 are shown in Fig. 4.6. Figure 4.6 (a) shows the microstructure and morphology of the Ti_2Cu phase along with α" and transformed β phase. Fig. 4.6 (b-d) shows the elemental distribution of titanium, copper, and niobium. All three elements are almost homogeneously distributed in the matrix, and EDS analysis at this place confirms the availability of both copper and niobium

along with titanium. Atomic and weight percent are shown in Fig. 4.6 (e).

Figures 4.7 and 4.8 are the EDS analysis and mapping of S3 and S4. The high niobium content and the corresponding change in the microstructure can be observed in Figures 4.7 (a) and 4.8 (a). In Fig. 4.7 (a), copper in flake form and niobium in laminate structure can be seen easily. The microstructure of alloys S3 and S4 was similar to previous research (Han et al., 2015; Ibrahim et al., 2018). Further, the presence of niobium and copper is confirmed by corresponding EDS analysis. Figure 4.8 (a) represents the microstructure of alloy S4, and the presence of maximum α" phase, β-phase along with Ti_2Cu is approved by the XRD analysis of the alloy. All the alloy's microstructure and EDS analysis agreed with the XRD pattern. The presence of a significant quantity of copper, the Ti_2Cu phase, and the β-phase also confirm the elemental distribution in the matrix.

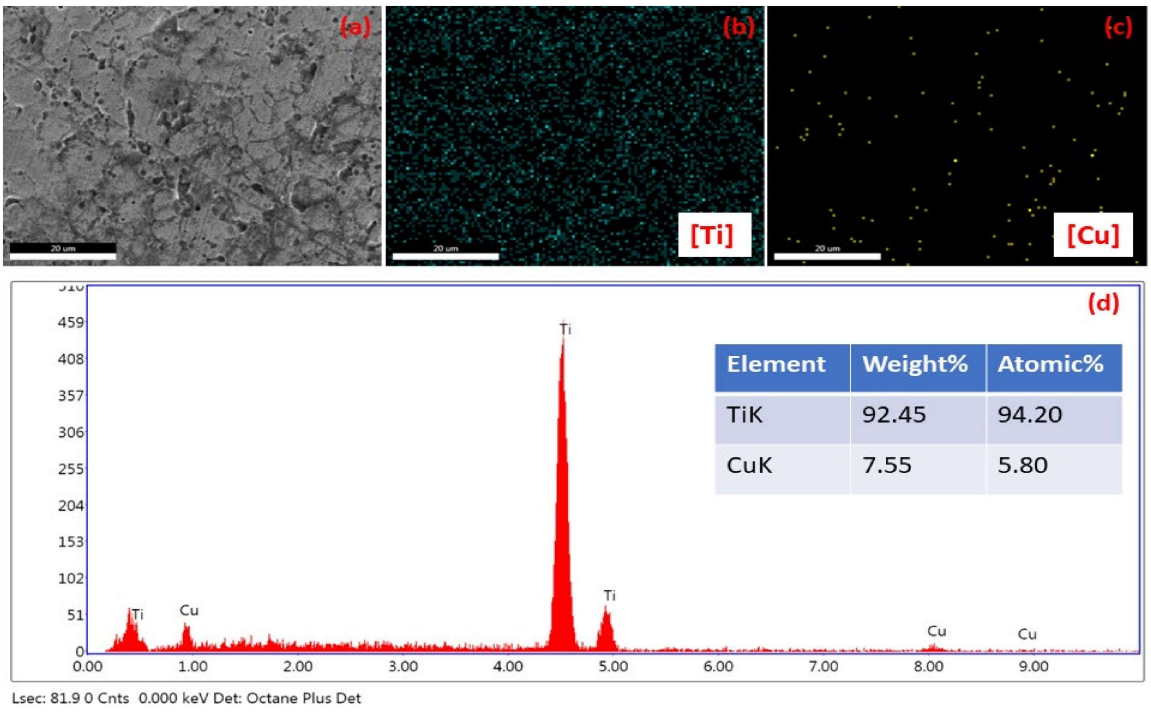

Fig. 4.5- The HR-SEM image (a), EDS map scanning image of Ti (b) and Cu (c), weight and atomic percent of element (d), and EDS point scanning pattern (e) of sintered alloy S1.

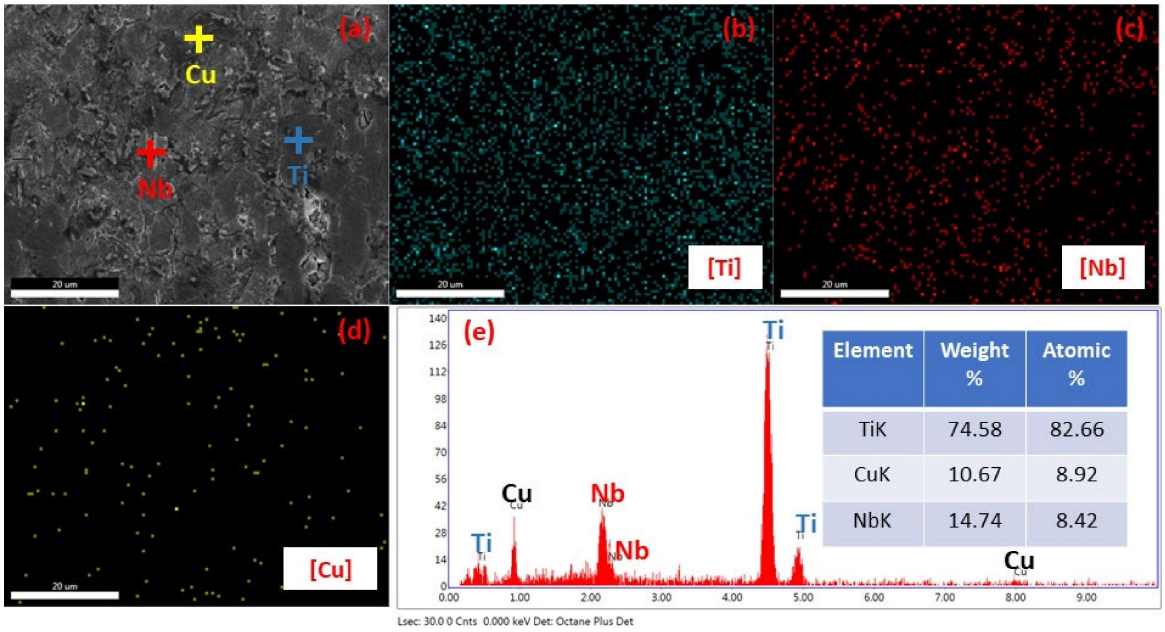

Fig. 4.6- The HR-SEM image (a), EDS map scanning image of Ti (b), Nb (c), Cu (d), and EDS scanning pattern (e) of sintered alloy S2.

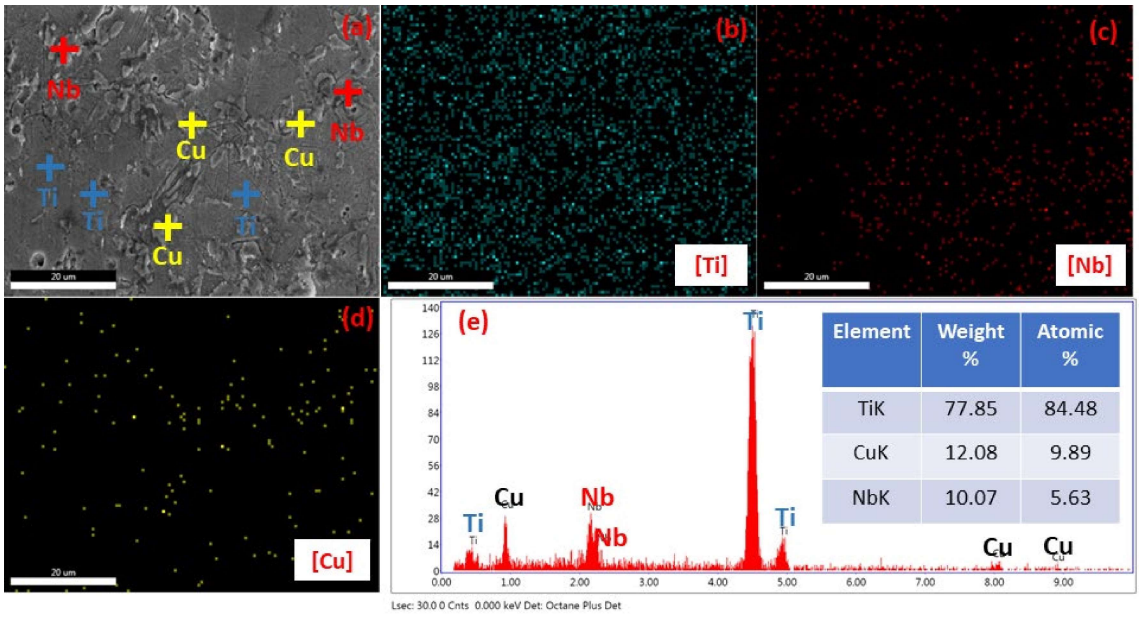

Fig. 4.7- The HR-SEM image (a), EDS map scanning image of Ti (b), Nb (c), and Cu (d), EDS point scanning pattern (e) of sintered alloy S3.

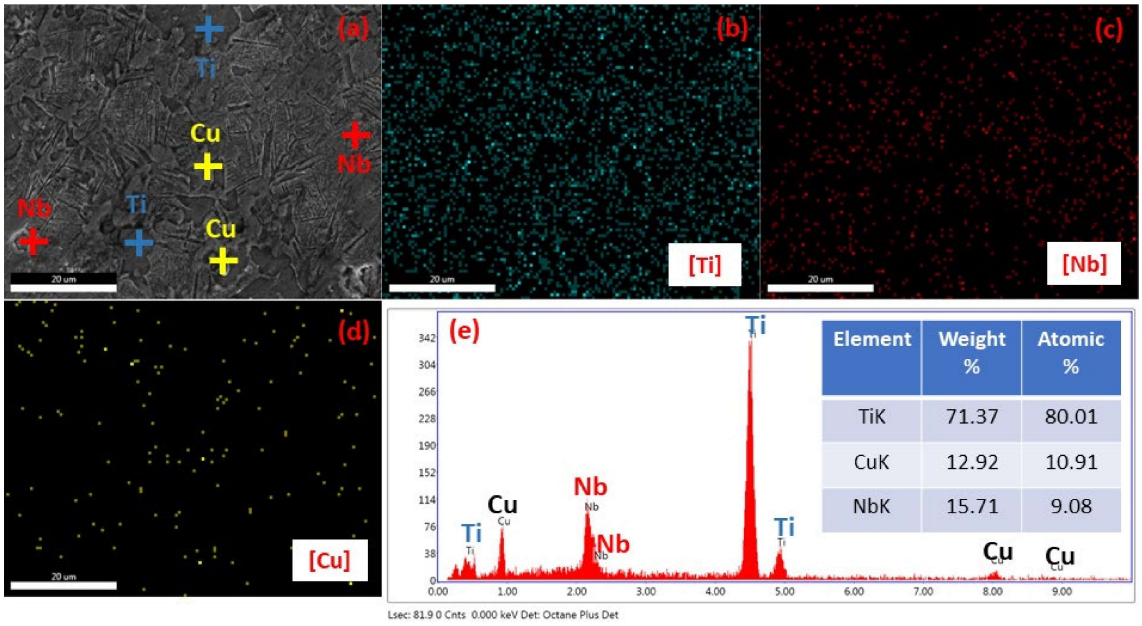

Fig. 4.8- The HR-SEM image (a), EDS map scanning image of Ti (b), Nb (c), and Cu (d), EDS point scanning pattern (e) of sintered alloy S4.

4.3 Physical and Mechanical properties

The theoretical and sintered density, micro-hardness, structural porosity, and compressive strength value of samples S1, S2, S3, and S4 are listed in Table 4.4. A comparison bar diagram of the theoretical and sintered density of the samples is shown in Fig. 4.9. It is observed that the sintered density of sample S1 is higher (99.35% to theoretical density) and gradually decreases to the lowest for S4 (89.94% to theoretical density). The Vickers micro-hardness value shown in Fig. 4.10 depicts that increasing porosity decreases the micro-hardness of the samples. The addition of niobium in the alloy decreases its sintered density because the melting point of niobium is much higher than both titanium and copper.

The micro-hardness value of samples S1, S2, S3, and S4, are 458±16.32, 541.8±16.28, 359±4.03, 267±12.25 respectively, which is much higher than CP-Ti. Liu et al. and Zhang E. et al. (J. Liu et al., 2014; E. Zhang et al., 2013) also reported a microhardness value of 160.3 of CP-Ti at the same parameter. The micro-hardness value of sample S2 is highest compared

to other samples. The addition of niobium reduces the sintered density, and similar behavior is reported when niobium is mixed with Ag in titanium (Shivaram et al., 2020). The inclusion of copper amplifies the micro-hardness of titanium (J. Liu et al., 2014). Therefore, all samples have more hardness than CP-Ti. Here, adding 5% niobium increases the hardness to a maximum level and decreases to a lower value for 15 % niobium (S4) because of lower density. So, samples S3 and S4 have lower hardness values than other samples. Similar behavior is reported in the literature when niobium with 10% and 15% alloyed with Ti-15Mo (L. B. Zhang et al., 2015).

Table 4.4- Micro-hardness (HV), density, porosity, and compressive strength of sintered alloys

Sample	Sintered density(gm/cc)	Theoretical density(gm/cc)	Structural Porosity (%)	Micro-hardness (HV)	Compressive strength (MPa)
S1	4.58±0.02	4.61	0.65±0.43	458±16.32	685±40
S2	4.67±0.03	4.73	1.26±0.63	542±16.28	1090±50
S3	4.62±0.02	4.85	4.74±0.21	359±14.03	816±60
S4	4.47±0.04	4.97	10.06±2.21	267±12.25	644±30

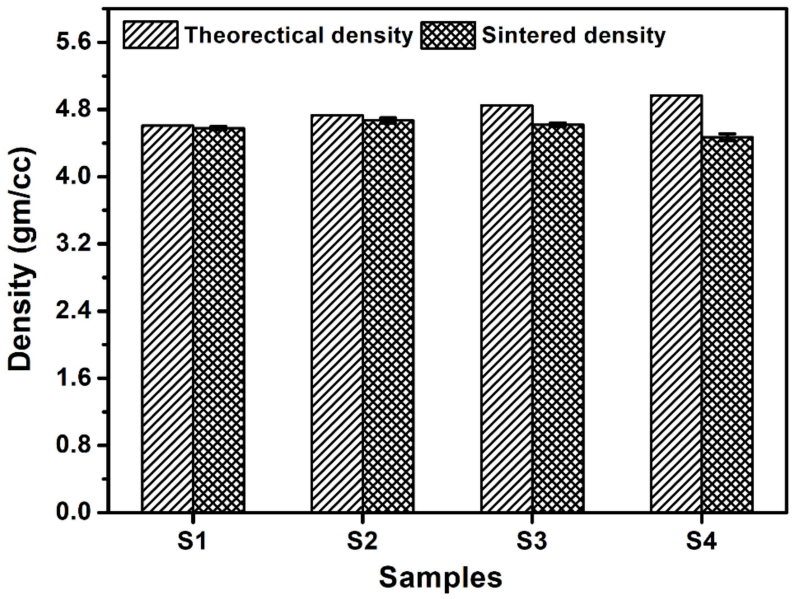

Fig. 4.9- comparison of the theoretical and sintered density of the alloys.

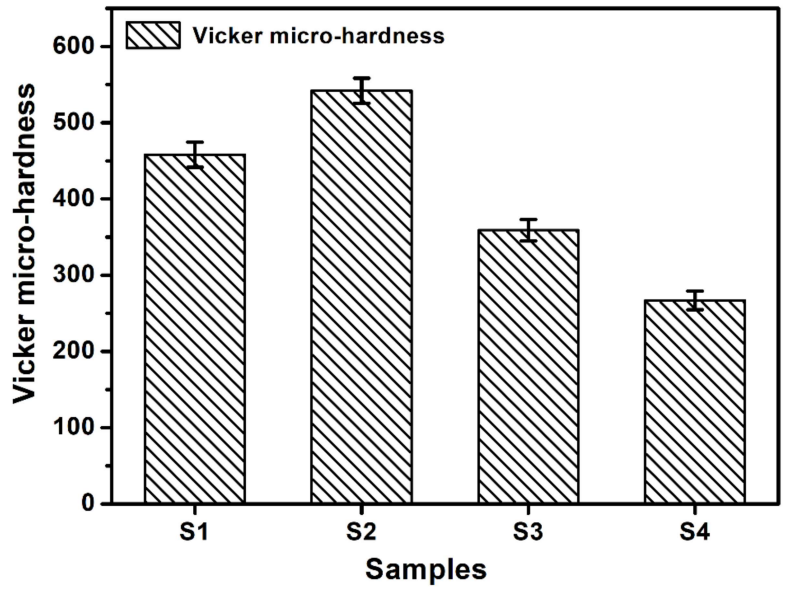

Fig. 4.10- Vickers micro-hardness of samples.

Figure 4.12 shows the compressive stress-strain plot for samples S1, S2, S3, and S4 obtained by compression test. The addition of niobium increases the yielding strain of the alloy. The biomaterial should have a high yield strength and low elastic modulus to avoid the stress shielding effect. The yield strain value increases with the addition of niobium and is maximum

for sample S4. The highest value of compressive strength is for sample S2 (1090MPa) and the lowest for sample S4 (644MPa), indicating that 5% niobium has better compressive strength than that of 10% and 15%. Niobium acts as a β- stabilizer element when alloyed with titanium. The β-phase of titanium has a BCC structure and is the reason for the suitable mechanical property. The different processing routes and new alloying elements are the main reason for the sintered alloy's higher compressive strength. Therefore, we can conclude that adding niobium to the Ti-5Cu alloy gives a better mechanical property.

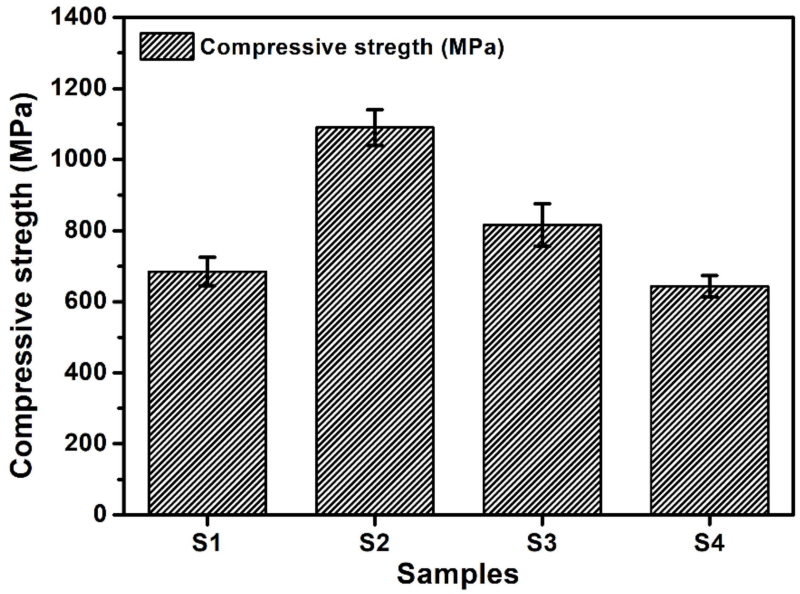

Fig. 4.11- Compressive strength value of samples observed after compression test.

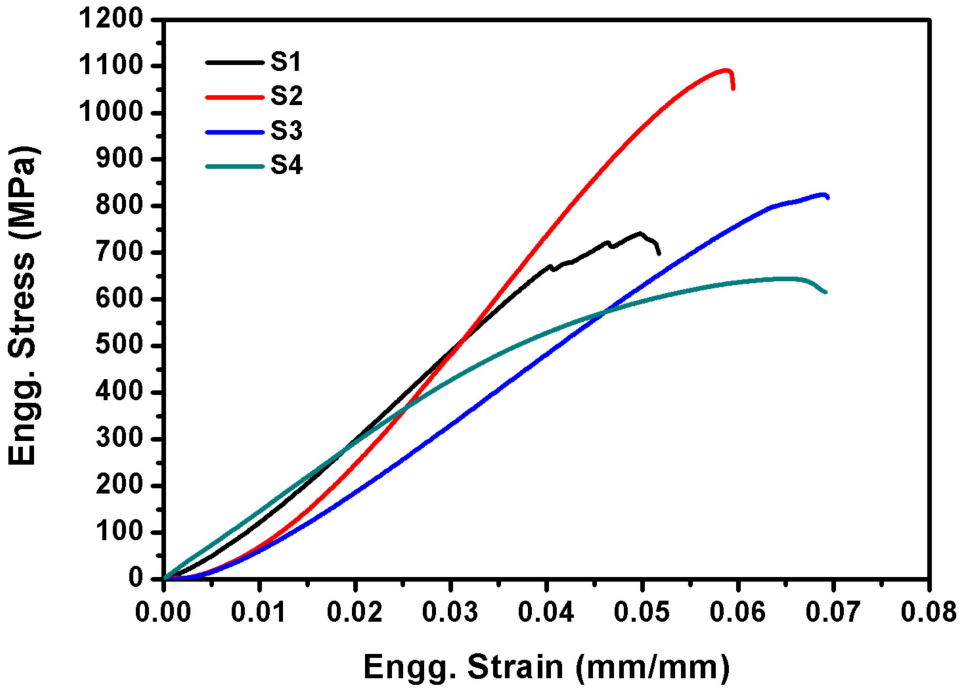

Fig. 4.12- Variation of Engineering stress with Engineering strain of alloys S1, S2, S3, and S4.